Leakage current measurements of CZT microstrip detectors

N. Auricchio[1], E. Caroli[1], F. Moscatelli[2], F. Schiavone[1], A. Basili[1]

Internal Report INAF/IASF-Bo n. 605/2012

Affiliation:

[1] INAF/IASF-Bo, via Gobetti 101, Bologna, Italy
[2]IMM/CNR, via Gobetti 101, Bologna, Italy

TABLE OF CONTENTS

Aims

This document describes the experimental set-up used at the IMM/CNR (Bologna) to carry out the leakage current measurements of the CZT strip detectors involved in the project *Development of an high efficiency wide band 3D CZT detector prototype for Laue telescope focal plane* and the related results. The aim of these measurements is to evaluate the functional characteristics of the detectors and their uniformity in terms of leakage current. These measurements will be repeated after the bonding realization indispensable to connect the electrodes to the metallic pads on the alumina support in order to compare the current values.

1. Summary

The objective of the project is to realize a 3D position sensitive prototype as focal plane detector for telescope based on wide band Laue lens. The prototype is based on the use of CZT crystals in the Planar Transverse Field (PTF) configuration, in which the direction of the incoming photons is perpendicular to the applied electrical field. This configuration allows increasing the photon absorption thickness to enhance the detection efficiency at high energy, without increasing the charge collection distance, avoiding spectroscopic performance degradation. The drawback of the PTF irradiating geometry is that all the positions between the collecting electrodes are uniformly hit by radiation leading to a stronger effect of the difference in charge collection efficiency in the spectroscopic performance with respect to the standard Parallel Planar Field (PPF) irradiation configuration through the cathode.

Therefore, in order to improve the CZT sensitive unit performance, we have decided to use an anode composed of an array of micro-strips in a drift configuration: a thin collecting anode strip surrounded by guard strips with decreasing bias voltage. This anode configuration, proposed and studied at NSI/DTU in Copenhagen [1], allows the detector to become almost a single charge carrier device, in which the signal depend only on the electron collection, avoiding the degradation of the spectroscopic response by the charge loss due to the hole trapping and providing a more uniform spectroscopic response, independent from the distance of the interaction from the collecting electrodes. In addition, it will possible to perform a further compensation of the collected charge signals using the photon interaction position that can be inferred by the ratio between the cathode and the anode strip signals.

Finally, in order to obtain 3D sensitivity for the photon interaction position, the cathode is segmented into four strips in the direction orthogonal to the anode ones. Therefore the final prototype becomes equivalent to a stack of thinner CZT horizontal layers with the advantage of not having any passive material between each layer [2,3,4].

This report describes the experimental set-up used to carry out the leakage current measurements on 6 CZT unbonded detectors during the test phase at IMM / CNR of Bologna and presents the results obtained.

The aim of these measurements is to evaluate the functional characteristics of the detectors and their uniformity in terms of leakage current, because these data were not provided by the manufacturer. These measurements will be repeated after the bonding procedure, indispensable to contact the electrodes to the metallic pads on the alumina support in order to check that the current values are not increased excessively.

2. Sensor sample main characteristics

The CZT sensors (Figure 1) were realized by Quik-Pak (CA, USA) cutting 8 single crystals of $19.35\times8\times2.4$ mm^3 from REDLEN Tech. (BC, Canada) CZT wafers. On the anode side, the microstrip set is divided in 8 equivalent pixels with a pitch of 2.4 mm, being only 8 strips connected to the readout electronics, while the others act as drift strips. Four drift strips on each side surround each collecting strip, with the central one shared. In total, the anode side is composed by 64 metallic (Ni/Au) µ-strips 0.15 mm wide with a gap of the same size. The cathode side is made by a set of

four metallic strips that are orthogonal to the anode ones with a pitch of 2 mm (1.9 mm wide Ni/Au metallisation with a 0.1 mm gap).
The number code of the detectors, together with some notes deduced from a visual inspection of the whole detector under a microscope, is shown in Table 1.

Detector Number code	**Notes**
2887A	☺
2887B	☺
3417A	☹, damaged by glue
3417B	😐, strip 63 bad cut, beveled edge
3660A	😐, beveled edge from strip 58, horizontal scrape on 7 strips at the detector centre
2081A	☺

Table 1. Number code of the detectors tested and related notes.

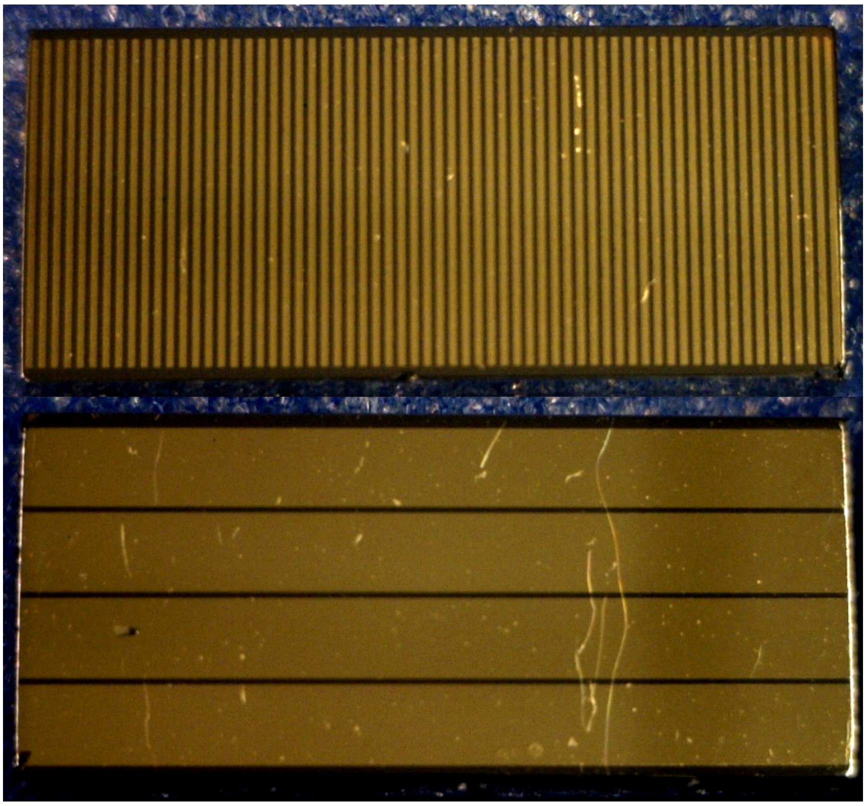

Figure 1. CZT anode side (top) and the cathode side (bottom).

3. Experimental set-up and measurement procedure

The total leakage current is determined by two important parameters, the bulk and surface conductivity, thus we have carried out both the surface and the bulk leakage current measurements. Low surface resistivity results in a high leakage current and it can also affect the electric field line distribution near the contacts, affecting the charge collection efficiency, in multi-contact CZT devices such as coplanar grid, strip and pixel detectors.

The main drawback of using the steering electrodes (or applying a differential bias) is the extra surface leakage current component that significantly increases the total leakage current and thermal noise. Thus, the total leakage current turns out to be more than the sum of two separately measured bulk and surface components.

The current-voltage I-V electrical measurements were performed using a computer controlled parametric characterization system. This is based on a semi-automatic probe station (Micromanipulator MM6620) with a Temptronic TP315B thermo chuck, a Keithley K707 switching matrix (equipped with 7072 and 7174 semiconductor cards) and a KeithleyK90 I-V measuring system, composed by a syncronization controller (K2361) and four source measure units (Keithley K238).

In the case of surface current, the voltage was applied to one strip while the other was kept at zero potential. These surface measurements have been applied to strip pairs located in five different areas of the crystal surface: at the centre, close to both ends of the detector and between these two regions. In Figure 2 on the left we report the photo of the CZT detector positioned on the adhesive blue foil, above the chuck in order to allow the perfect adherence after activating the vacuum to avoid possible displacements caused by vibrations, while on the right we can note the selected strips contacted through the use of microprobes (attached to the manipulators). The bias voltages ranges from -100V to 100V in steps of 1 V.

In the case of bulk current, we have taken two kinds of measurements, one in which the voltage source was applied to the cathode by an Aluminum support biased from a microprobe, while a strip was kept at zero potential, from which the bulk current was measured, and the other one in which the anode side was on the Al support at 0HV by a microprobe and the bulk leakage current was measured on the cathode with 4 microprobes connected to the same bias voltage supply, as displayed in Figure 3, where the sensor anode side is located on the Al support, that is biased at ground potential by a microprobe, and four microprobes are used to connect the 4 cathodes. The bias voltages ranges from -100V to 100V in steps of 1 V.

The measurements, starting at -100V for bulk current or at -50V for surface current, have been taken after a initial delay of 5 s to allow the stabilization of the electric field and the time interval between the application of each bias voltage and the current measure is 1 s. When changing the voltage polarity, the delay is 5 s in order to avoid the influence of transient effects.

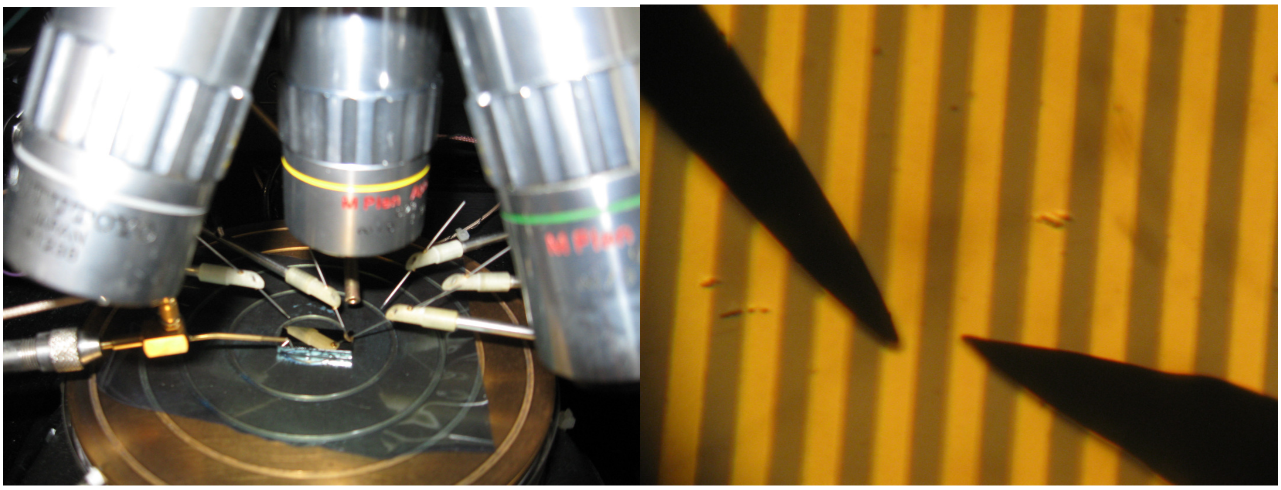

Figure 2. On the left: photo of the CZT detector positioned on the chuck of the probe station. On the right: two selected strips contacted through the use of microprobes.

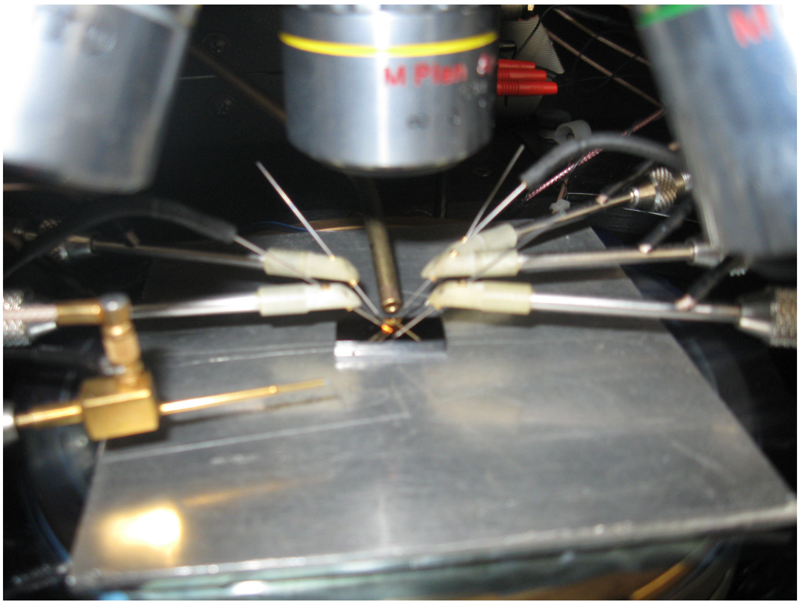

Figure 3. Sensor anode side located on the Al support, biased at ground potential, and four microprobes used to connect the 4 cathodes.

4. Measurement results

In the following sections we report the results of the leakage current measurements.

4.1 Bulk leakage currents

In Figure 4 we illustrates the measurements of the bulk leakage current acquired for all unbounded detectors in the configuration in which all the strips are at ground potential and the bulk current is measured by four microprobes connected to four cathodes, biased from -100V to 100V, while in table 2 we report the current values at ±100V.

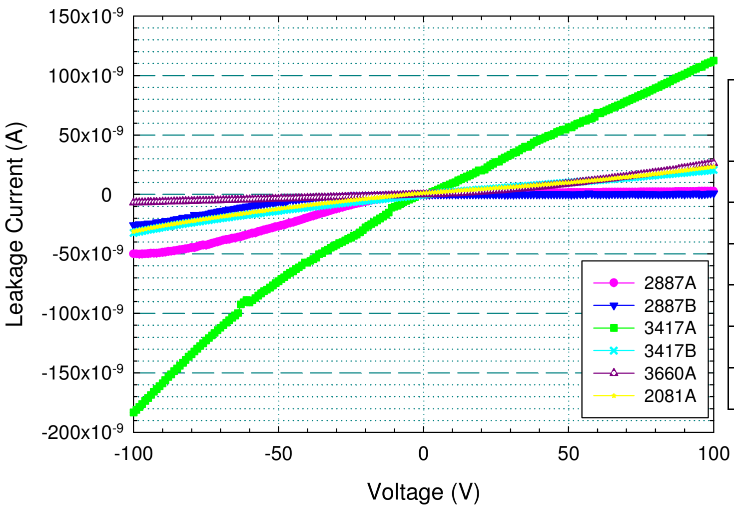

Figure 4. All bulk leakage current.

Detector number code	Value at -100 V (nA)	Value at 100 V (nA)
2887A	-50.00	2.69
2887B	-25.70	1.02
3417A	-183.00	113.00
3417B	-32.20	20.60
3660A	-6.93	26.20
2081A	-31.10	23.40

Table 2. Bulk leakage current values.

In Figure 5 the measurements of the bulk leakage current are reported, obtained for all unbounded detectors in the configuration in which the cathodes are biased from -100V to 100V and one strip is held at zero potential.

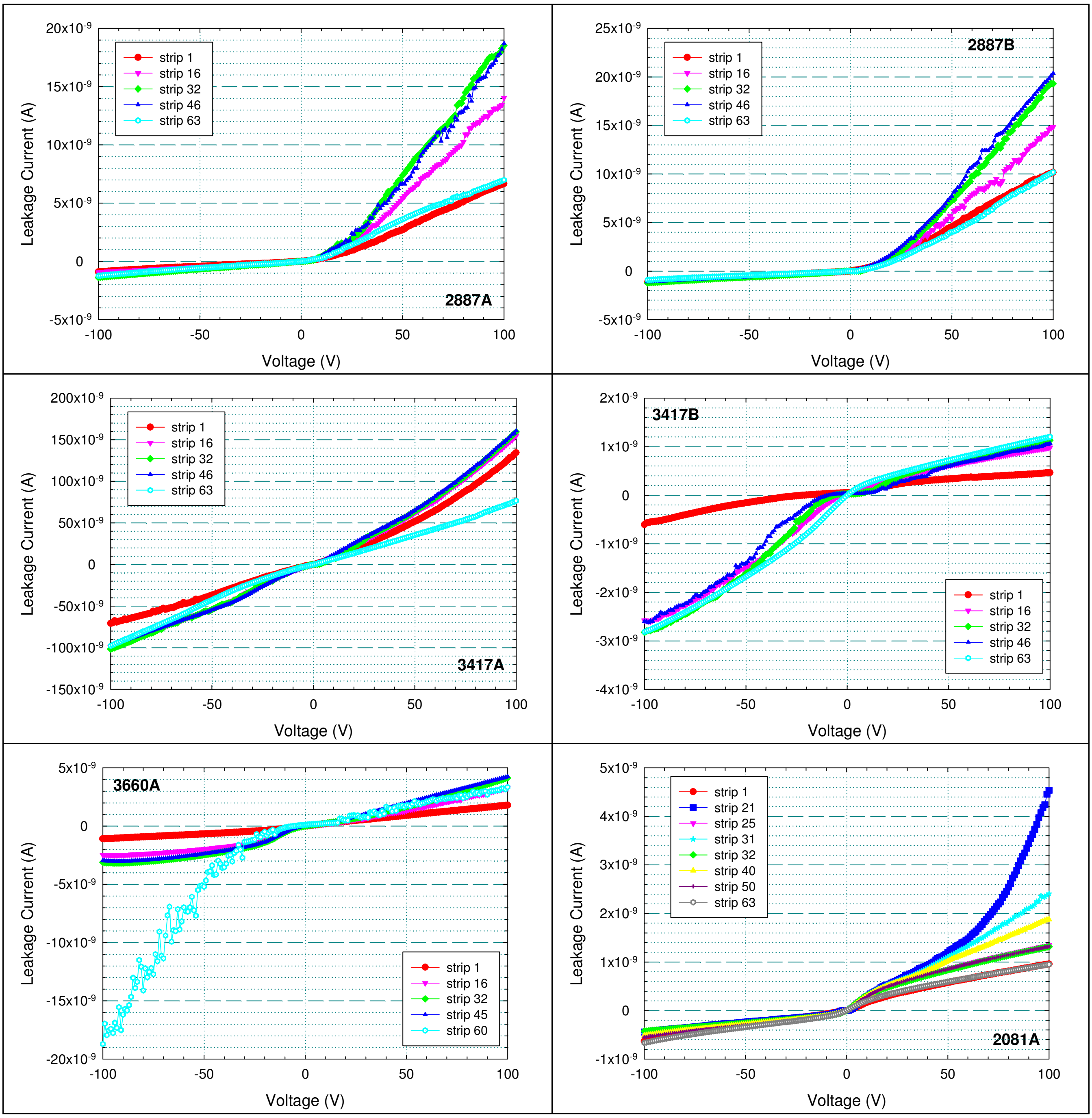

Figure 5. Strip bulk leakage current.

In table 3 the mean values of current calculated at ±100V for the measured strips are summarized.

Detector number code	Mean value at -100 V (nA)	Mean value at 100 V (nA)
2887A	-1.15±0.22	13.0±5.9
2887B	--1.09±0.12	15.0±4.8
3417A	-93.2±12.7	137±35
3417B	-2.29±0.94	1.0±0.3
3660A	-5.66±1.33	3.36±0.98
2081A	-0.53±0.1	1.84±0.57

Table 3. Mean values of the bulk leakage current measured on the strips held to ground potential and calculated at ±100V.

Regarding to the detector 2081A, in Figure 6 we report the comparison between two subsequent measurements on the strip 63: the second I-V characteristic was taken after we noticed some scratches on the cathode surface (see Figure 1, bottom). The current is not worse as a result of these surface scratches, on the contrary it is improved, due to more time spent in the dark inside the probe station.

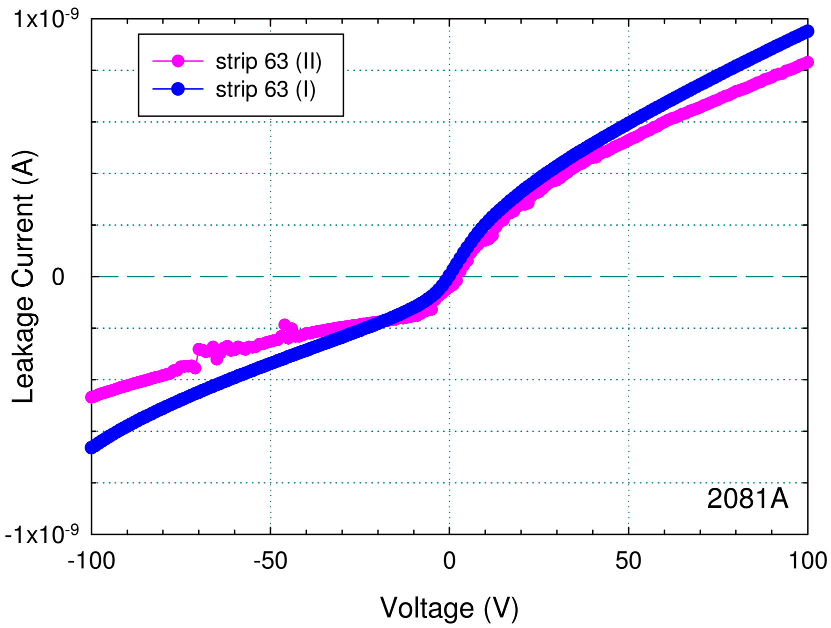

Figure 6. Comparison between two I-V characteristics acquired on the strip 63 of 2081A detector.

4.2 Surface leakage currents

In Figure 7 the measurements of the surface leakage current are displayed for some tested strip pairs.

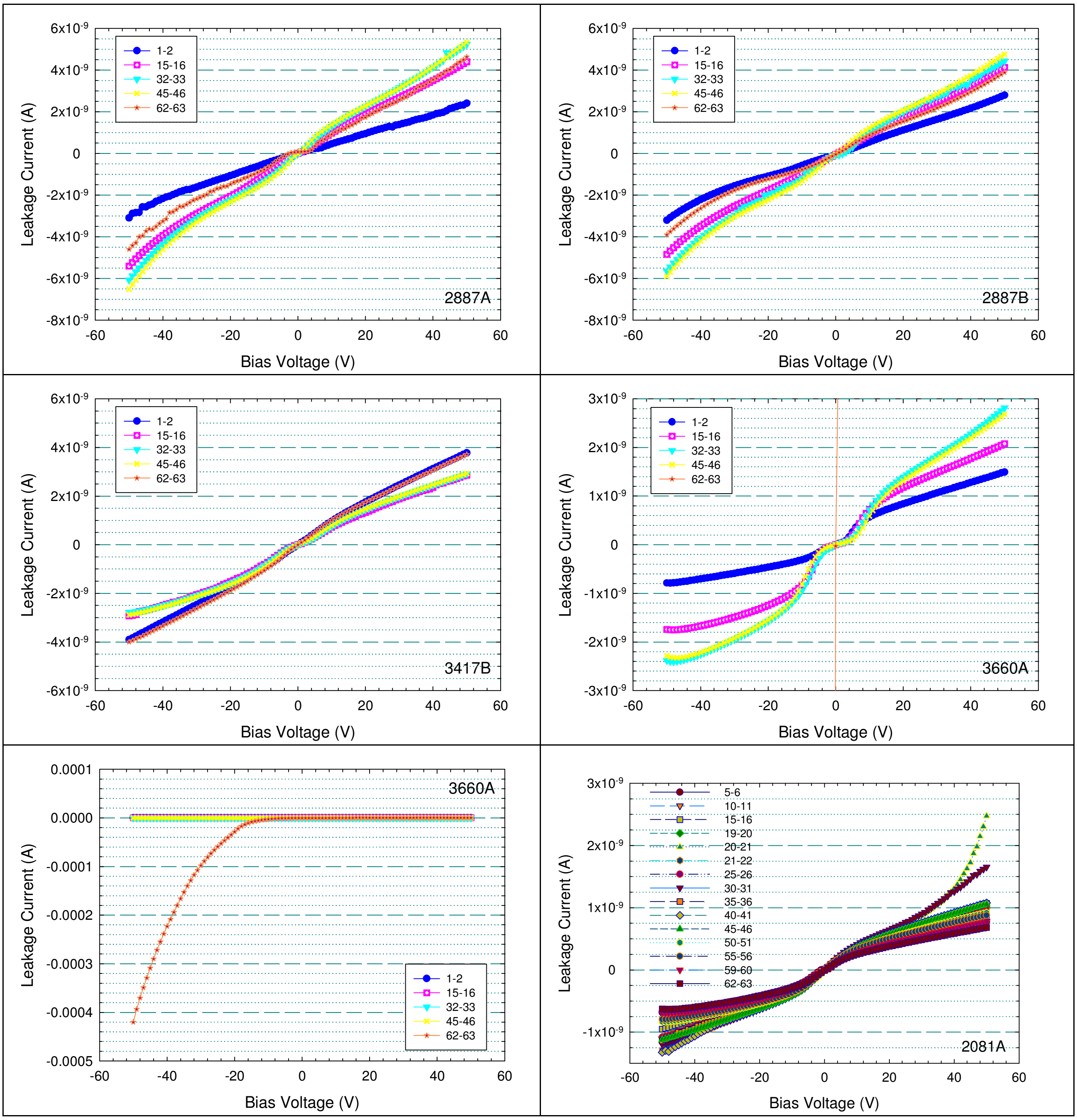

Figure 7. Surface bulk leakage current.

Regarding to the detector 2081A, we can note that the current between the strips 20 and 21 is 2.5 times greater than that measured on the neighbouring strips as a consequence of deep scratches in the gap between the strips (see Figure 2, right). The current between the strips 30 and 31 is a bit higher than the other because of a scratch on the strip 31.

Figure 8 shows the distribution of surface leakage current measured between strip couples on the anode side for 4 CZT sensors. The measured strip's couples represent a significant sample of the anode strip set and they were taken mainly at five different regions of the crystal surface: close to both ends, centre and between these two regions. The distribution shape is due to the surface leakage current values, that normally increase from centre to ends: for strip couples close to sensor ends the measured leakage currents are up to 50% higher with respect to the centre region.

Finally in table 4 the mean values of the current calculated at ±50V are reported.

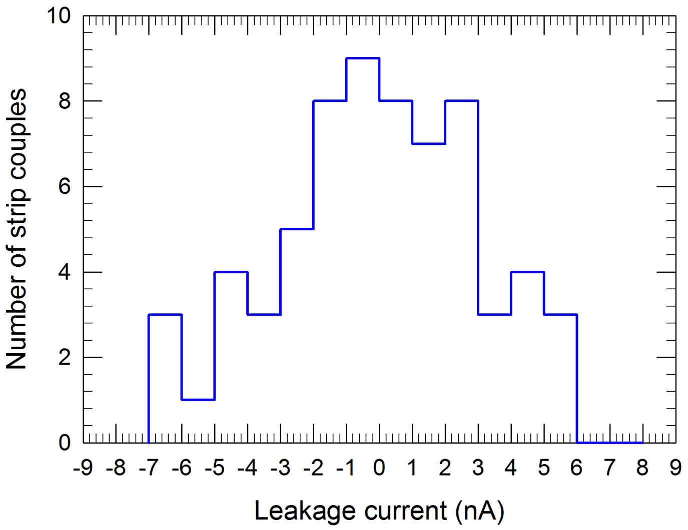

Figure 8. Distribution of the surface leakage current for a representative set of the anode side strips in 4 CZT sensors.

Detector number code	Mean value at -50 V (nA)	Mean value at 50 V (nA)
2887A	-5.1±1.3	4.4±1.2
2887B	-4.7±1.1	4.0±0.8
3417A	noisy	noisy
3417B	-3.3±0.6	3.2±0.5
3660A	$(-8.4\pm1.9)10^4$	74.2±16.1
2081A	-1.0±0.2	1.1±0.5

Table 4. Mean values of the surface leakage current at ±50V for 5 detectors.

5. Current measurements on the detector supports

In order to check the insulation among the metallic traces that feed the drift strips by voltage divider, realized by means of the dielectric DuPont QM44 (in dark green in Figure 9), thick (30±2) µm, we have measured the current flowing between the 1-2, 2-3, 3-4, 4-5 bonding pad pairs, where the pad 5 is the anodic strip.

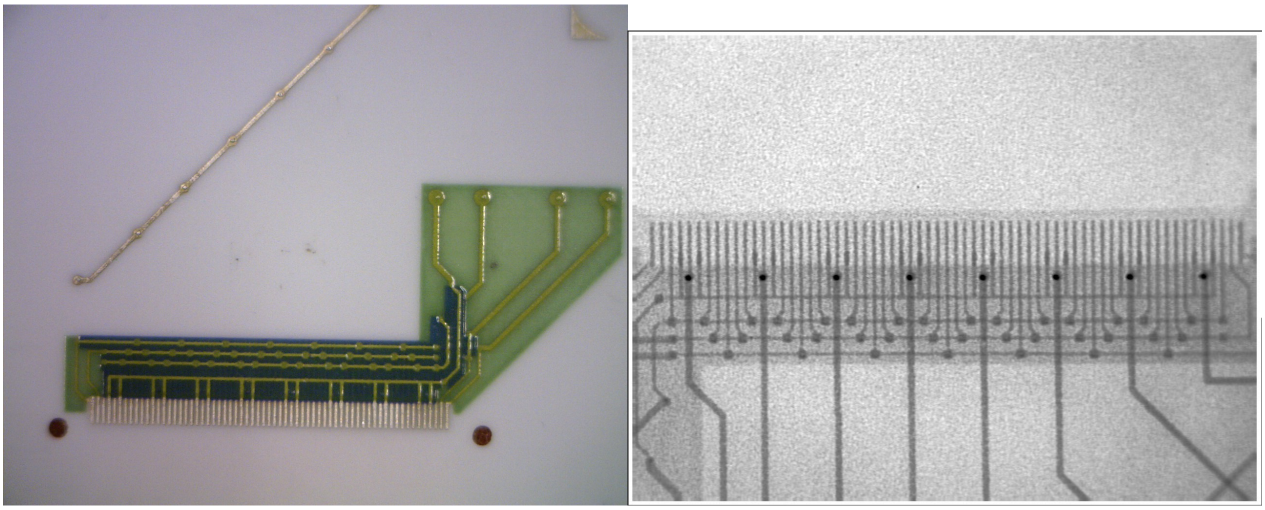

Figure 9. Detector support: anode side (left), radiographic image at X-rays (right).

In following figure the current measured between the pad couples on eight supports is shown.

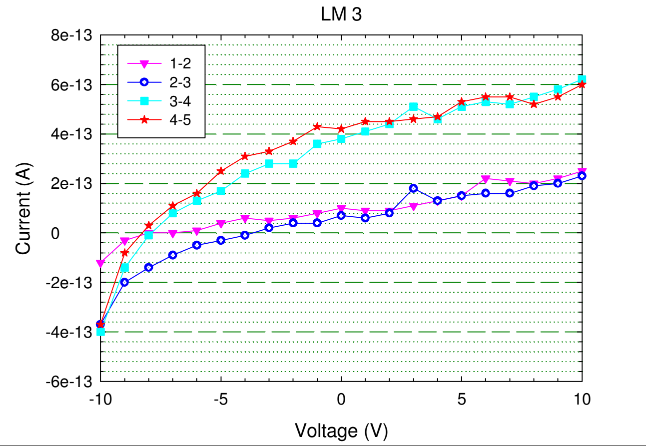
LM 3
Current (A)
8e-13
6e-13
4e-13
2e-13
0
-2e-13
-4e-13
-6e-13
-10
-5
0
5
10
Voltage (V)
1-2
2-3
3-4
4-5

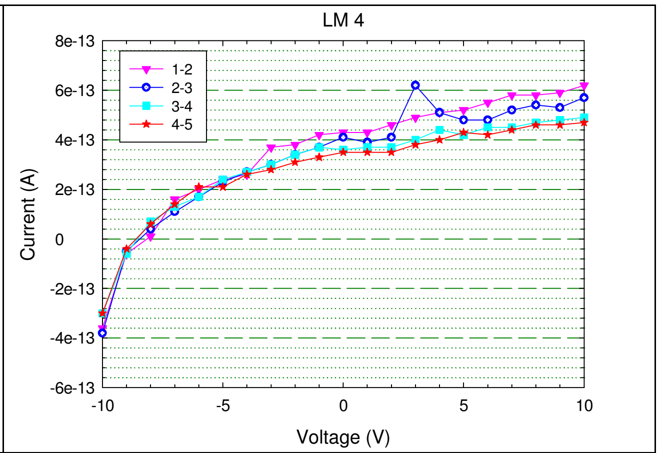
LM 4
Current (A)
8e-13
6e-13
4e-13
2e-13
0
-2e-13
-4e-13
-6e-13
-10
-5
0
5
10
Voltage (V)
1-2
2-3
3-4
4-5

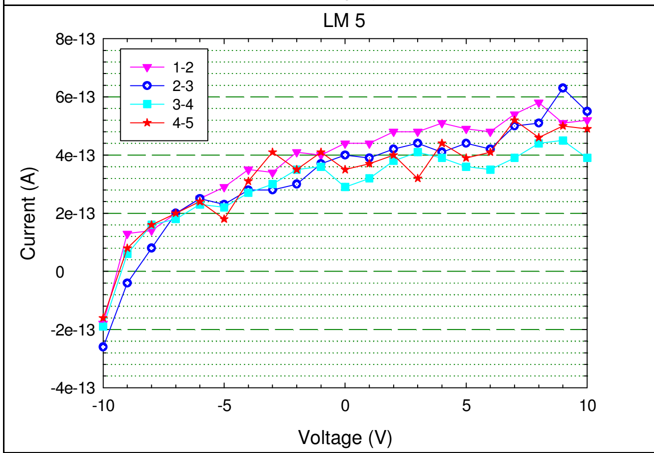
LM 5
Current (A)
8e-13
6e-13
4e-13
2e-13
0
-2e-13
-4e-13
-10
-5
0
5
10
Voltage (V)
1-2
2-3
3-4
4-5

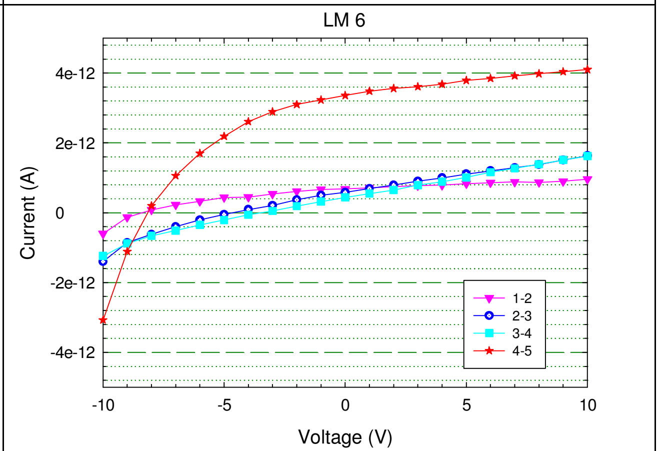
LM 6
Current (A)
4e-12
2e-12
0
-2e-12
-4e-12
-10
-5
0
5
10
Voltage (V)
1-2
2-3
3-4
4-5

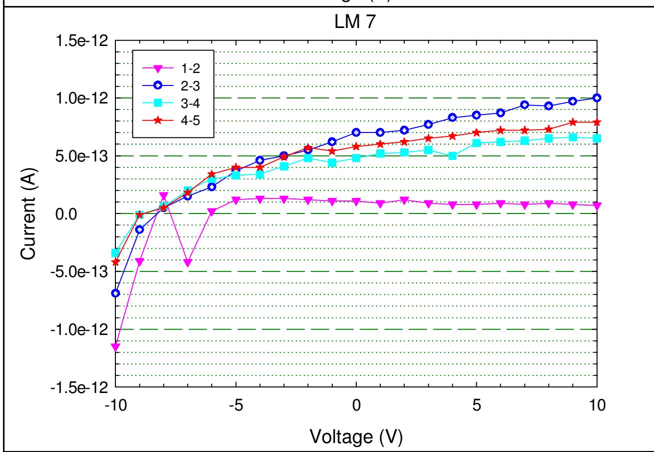
LM 7
Current (A)
1.5e-12
1.0e-12
5.0e-13
0.0
-5.0e-13
-1.0e-12
-1.5e-12
-10
-5
0
5
10
Voltage (V)
1-2
2-3
3-4
4-5

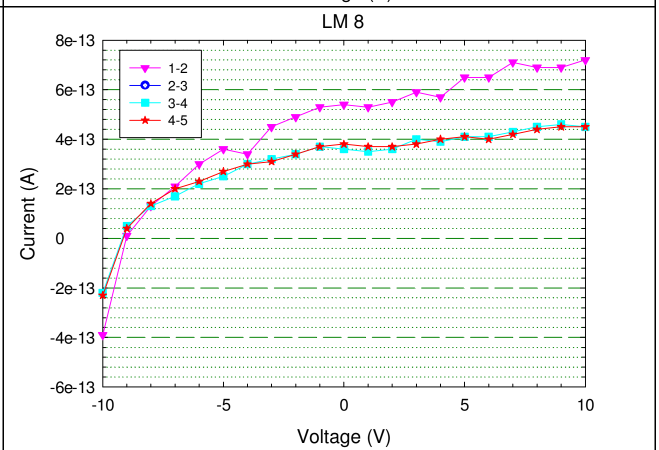
LM 8
Current (A)
8e-13
6e-13
4e-13
2e-13
0
-2e-13
-4e-13
-6e-13
-10
-5
0
5
10
Voltage (V)
1-2
2-3
3-4
4-5

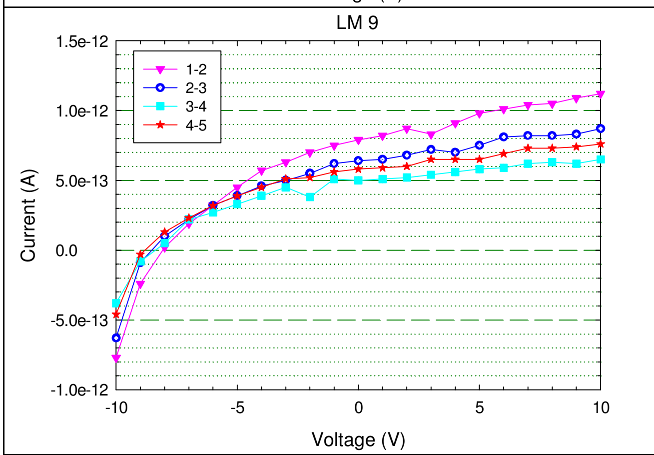
LM 9
Current (A)
1.5e-12
1.0e-12
5.0e-13
0.0
-5.0e-13
-1.0e-12
-10
-5
0
5
10
Voltage (V)
1-2
2-3
3-4
4-5

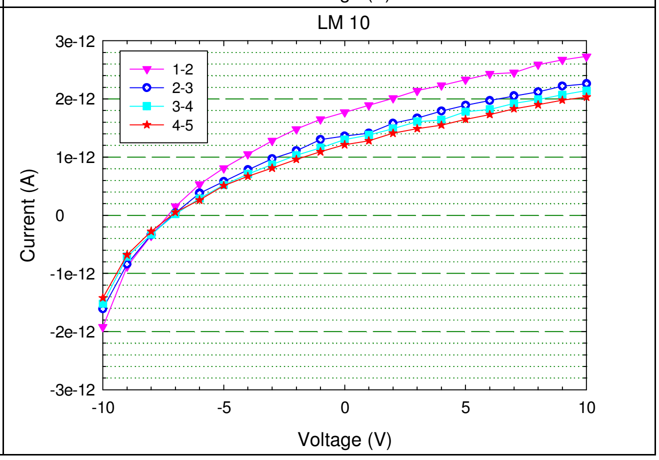
LM 10
Current (A)
3e-12
2e-12
1e-12
0
-1e-12
-2e-12
-3e-12
-10
-5
0
5
10
Voltage (V)
1-2
2-3
3-4
4-5

Figure 10. Currents between the 1-2, 2-3, 3-4, 4-5 bonding pad pairs of eight detector supports.

We can infer the cross currents are always below 4 pA, while we measured current values much higher in the supports 1 and 2 between several bonding pad couples, reported in table 5, and sometimes comparable to the leakage current of the strips. We are investigating the reason, probably because, being the first, the process was not yet fully operative.

	Support 1	**Support 2**
	Current at 10 V (A)	Current at 10 V (A)
bonding pad 1-2	$3.97\ 10^{-09}$	$2.15\ 10^{-10}$
bonding pad 2-3	$1.14\ 10^{-08}$	$4.14\ 10^{-10}$
bonding pad 3-4	$8.84\ 10^{-09}$	$3.35\ 10^{-10}$
bonding pad 4-5		$1.12\ 10^{-10}$
bonding pad 1-4	$2.42\ 10^{-09}$	$1.91\ 10^{-10}$
bonding pad 4-6	connected	connected
bonding pad 4-7	$9.11\ 10^{-09}$	
bonding pad 5-6	$1.78\ 10^{-10}$	
bonding pad 5-7	$1.78\ 10^{-10}$	
bonding pad 6-7	$8.51\ 10^{-09}$	

Table 5. Measured currents flowing between bonding pad couples.

7. Conclusions

We have measured the surface and bulk leakage currents of six CZT microstrip crystals, only one presents very high current values because it was damaged by the glue used in a preliminary bonding phase to connect the strips to the pads on the detector supports.
We have also controlled the insulation realized by means of a thin dielectric layer between the metallic traces that supply the drift strips on the detector supports.

References

1) Van Pamelen, M.A.J., Budtz-Jørgensen, C. and Kuvvetli, I.
"Development of CdZnTe X-ray detectors at DSRI" .
Nucl. Instr. and Meth. in Phys Res. A 439, 625-633 (2000).

2) E. Caroli, N. Auricchio, S. del Sordo, L. Abbene, C. Budtz-Jørgensen, F. Casini, R. M. Curado da Silva, I. Kuvvetli, L. Milano, L. Natalucci, E. M. Quadrini, J. B. Stephen, P. Ubertini, M. Zanichelli, A. Zappettini.
"Development of a 3D CZT detector prototype for Laue Lens telescope".
High Energy, Optical, and Infrared Detectors for Astronomy IV, edited by Andrew D. Holland, David A. Dorn Proc. of SPIE Vol. 7742, pp. 77420V-1/77420V-9 (2010). doi: 10.1117/12.858120.

3) N. Auricchio, A. Basili, E. Caroli, C. Budtz-Jorgensen, R. M. Curado da Silva, S. Del Sordo, I. Kuvvetli, A. Mangano, L. Milano, L. Natalucci, E. M. Quadrini, J. B. Stephen, M. Zanichelli, A. Zappettini.
"A CZT High Efficiency Detector with 3D Spatial Resolution for Laue Lens Applications".
Nuclear Science Symposium Conference Record 2010, pp. 3683 - 3688.

4) I. Kuvvetli, C. Budtz-Jørgensen, E. Caroli, N. Auricchio.
"CZT Drift Strip Detectors for High Energy Astrophysics".
Nuclear Instruments and Methods in Physics Research A, 624 (2010), pp. 486–491.